

Technical Paper

**Hydrodynamic Forces for Heaving Cylinders
on Water of Finite Depth**

by

J.H. Hwang*, K. P. Rhcc*

and

Hisaaki Maeda**, Sumihiro Eguchi**

Abstract

A numerical method for solving the boundary-value problem related to potential flows with a free surface and an experimental work are introduced in this paper. The forced heaving motion of cylinders with arbitrary shapes in water of finite depth are considered here. The Fredholm integral equation of the first kind is employed in determining strengthes of singularities distributed on the body surface. And the results obtained by the present method for the case of a heaving circular cylinder on water of finite depth agree well with existing results of earlier investigators.

1. Introduction

Hydrodynamic forces, such as added mass, damping etc. for forced heaving cylinders in water of finite depth were investigated earlier by Yu & Ursell in 1961[1] and C.H. Kim in 1969[2]. They solved the boundary value problem related to the above problems by using multipole expansion method. In the present paper, the integral equation method by distributing singularities on the body surface has been developed to solve the same problem for cylinders of the arbitrary section.

This work has been performed by the joint research between the Seoul National University and the University of Tokyo. The analytical work has been done at the Seoul National University and the experimental work at the University of Tokyo.

2. Fundamental Equations.

For the coordinate system right-handed rectangular coordinate is used. The y axis is taken directed to the force of gravity, the x axis coincides with the free surface when the fluid is at rest and is taken directed to the left, as shown in Fig. 1. The normal vector,

n , at the contour of arbitrary section, C , is directed to the fluid, and h denotes the depth of water.

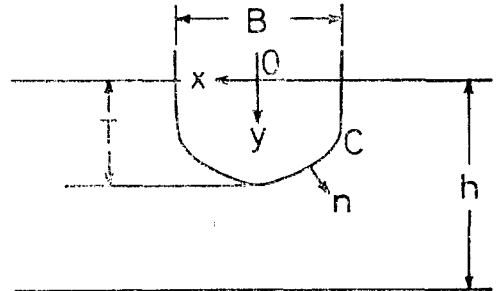


Fig. 1. Coordinate system

If the motion is started from the rest in the fluid of inviscid, incompressible and surface tension may be neglected, then the velocity potential Φ can exist.

Let P and η be pressure and elevation of free surface with time factor respectively. Now Φ , P and η can be rewritten as follows,

$$\Phi = R_e \{ \varphi e^{-i\omega t} \}, \tag{2.1}$$

$$P = R_e \{ p e^{-i\omega t} \}, \tag{2.2}$$

$$\eta = R_e \{ \eta e^{-i\omega t} \}, \tag{2.3}$$

Let

$$\varphi = i\omega Y \phi, \tag{2.4}$$

where Y is the amplitude of oscillation, and ϕ is

Presented at the Spring Meeting of the Society of Naval Architects of Korea Pusan, April 9, 1976.

* Member; Dept. of Naval Architecture, Seoul National University.

** Visitor; Institute of Industrial Science, University of Tokyo.

the velocity potential of unit velocity amplitude which must satisfy the Laplace equation

$$\frac{\partial^2 \phi}{\partial x^2} + \frac{\partial^2 \phi}{\partial y^2} = 0 \text{ in the fluid region,} \quad (2.5)$$

and also satisfy the following boundary conditions;

The linearized free surface condition

$$\frac{\partial \phi}{\partial y} + K\phi = 0 \quad \text{on } y=0, \quad (2.6)$$

where

$K = \omega^2/g$, g is gravitational acceleration.

Bottom condition

$$\frac{\partial \phi}{\partial y} = 0 \quad \text{on } y=h \quad (2.7)$$

Radiation condition

$$\phi \sim -iA^\pm(k_o) \cosh k_o(h-y) e^{\pm ik_o x} \text{ as } x \rightarrow \pm\infty, \quad (2.8)$$

where $A^\pm(k_o)$ is a Kochin function, and k_o is a positive root of

$$K = k_o \tanh k_o h. \quad (2.9)$$

Body boundary condition for heaving oscillation is

$$\frac{\partial \phi}{\partial n} = -\frac{\partial y}{\partial n} \quad \text{on } C, \quad (2.10)$$

and this condition can be rewritten by using stream function ψ instead of ϕ , as follows

$$\psi = x \quad \text{on } C, \quad (2.11)$$

Pressure equation can be derived from the Euler's equation of motion as follows

$$p = -\rho \omega^2 Y \phi. \quad (2.12)$$

The hydrodynamic forces can be obtained by integrating Eq. (2.12) along the body surface.

3. The velocity potential of unit strength by pulsating sources

Assume the velocity potential $\Phi(x, y, t)$ which is the solution of Laplace equation as

$$\Phi(x, y, t) = \log \frac{r}{r_1} \cos \omega t + \phi_1(x, y) \cos \omega t + \phi_2(x, y) \sin \omega t, \quad (3.1)$$

where r and r_1 are distances from the arbitrary point, $A(x, y)$, to the position of source, $S(a, b)$, and to the position of image of source about x -axis, $S'(a, -b)$, respectively.

$\phi_1(x, y)$ which can be determined to satisfy the free surface condition (2.6) and the bottom condition (2.7)

with $\log \frac{r}{r_1}$ is obtained as

$$\phi_1(x, y) = P.V. \int_0^\infty \left[\frac{2 \cos k h (h-b) \cosh k (h-y)}{\cosh k (K \cosh k h - k \sinh k h)} - \frac{2e^{-kh} \sinh k h}{k \cosh k h} \sin h k y \right] \cdot \cos k |x-a| dk, \quad (3.2)$$

where $P.V. \int_0^\infty$ represents the principal value integral, which must be taken to avoid a pole which exists on the path of integrating.

After performing the principal value integral along the path as shown in Fig. 2, we can obtain ϕ_1 as

$$\begin{aligned} \phi_1(x, y) = & 4\pi \frac{\cosh k_o (h-b) \cosh k_o (h-y)}{2k_o h + \sinh 2k_o h} \sin k_o |x-a| \\ & - \sum_{n=1}^\infty 4\pi \frac{\cos k_n (h-b) \cos k_n (h-y)}{2k_n h + \sin 2k_n h} e^{-k_n |x-a|} \\ & + R_e \left\{ P.V. \int_0^\infty \left[\frac{2 \cosh ik (h-b) \cosh ik (h-y)}{\cosh ik h (K \cosh ik h - ik \sinh ik h)} \right. \right. \\ & \left. \left. - \frac{2e^{-ikh} \sinh ik h}{ik \cosh ik h} \sin h ik h \right] e^{-k |x-a|} |dk \right\}, \quad (3.3) \end{aligned}$$

where k_n are positive roots of the following equation

$$K \cos k_n h + k_n \sin k_n h = 0. \quad (3.4)$$

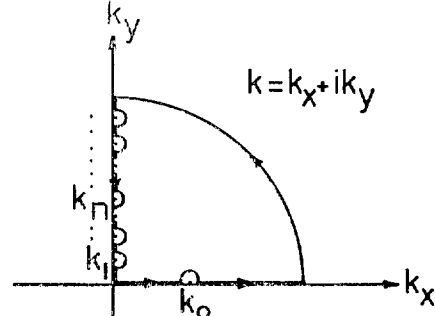


Fig. 2. Integrating path

After Substituting Eq. (3.3) into Eq. (3.1), we can determine the $\phi_2(x, y)$ from the radiation condition (2.8) as

$$\phi_2(x, y) = -4\pi \frac{\cosh k_o (h-b) \cosh k_o (h-y)}{2k_o h + \sinh 2k_o h} \cos k_o |x-a| \quad (3.5)$$

Finally, the solution of Laplace equation which satisfies all boundary conditions can be rearranged as

$$\begin{aligned} \Phi(x, y, t) = & 2\pi \frac{k_o^2 - K^2}{k_o (hk_o^2 - hK^2 + K)} \cosh k_o (h-b) \cosh \\ & k_o (h-y) \sin(k_o |x-a| - \omega t) \\ & - \sum_{n=1}^\infty 2\pi \frac{k_n^2 + K^2}{k_n (hk_n^2 + hK^2 - K)} \cos k_n (h-b) \cos k_n (h-y) \\ & e^{-k_n |x-a|} \cos \omega t. \quad (3.6) \end{aligned}$$

And the stream function, Ψ , which is a conjugate function of velocity potential, Φ , can be obtained as follows by Cauchy-Riemann-Condition,

$$\begin{aligned} \Psi(x, y, t) = & \text{sgn}(x-a) \left\{ -2\pi \frac{k_o^2 - K^2}{(k_o h k_o^2 - hK^2 + K)} \cosh \right. \\ & k_o (h-b) \sinh k_o (h-y) \cos(k_o |x-a| - \omega t) \\ & \left. - \sum_{n=1}^\infty 2\pi \frac{k_n^2 + K^2}{k_n (hk_n^2 + hK^2 - K)} \cos k_n (h-b) \sin k_n (h-y) \right\} \end{aligned}$$

$$e^{-k_0|x-a|\cos\omega t} \tag{3.7}$$

where $\text{sgn}(x-a) = \begin{cases} +1; x > a \\ -1; x < a \end{cases}$

4. Hydrodynamic forces

Since the Green function G at point $A(x,y)$ due to a source of pulsating strength at point $S(a,b)$ is equivalent to Eq.(3.6), the velocity potential at point A can be expressed in the form

$$\phi(A) = \frac{1}{2\pi} \int_c \left(\frac{\partial\phi(S)}{\partial n} - \phi(S) \frac{\partial}{\partial n} \right) G(A;S) ds. \tag{4.1}$$

Supposing $\sigma(S)$ as the strength of distributed sources over the section surface at point S , above equation can be rewritten as follows

$$\phi(A) = \int_c \sigma(S) G(A;S) ds(S), \tag{4.2}$$

and, from the body boundary condition, strength σ can be determined as a solution of Fredholm's integral equation of second kind. But, Eq. (4.2) can be changed as

$$\Psi(A)|_{\text{on } c} = \int_c \sigma(S) \bar{G}(A;S) ds(S) \tag{4.3}$$

by using stream function Ψ and conjugate Green function \bar{G} instead of ϕ and G respectively.

Let subscript c and s denote the real part and imaginary part of complex values respectively, then the body boundary condition (2.11) takes the following form.

$$\Psi_c|_{\text{on } c} = x \tag{4.4}$$

$$\Psi_s|_{\text{on } c} = 0 \tag{4.5}$$

And Eq.(4.3) can be divided into two parts.

$$x = \int_c (\sigma_c \bar{G}_c - \sigma_s \bar{G}_s) ds \tag{4.6}$$

$$0 = \int_c (\sigma_s \bar{G}_c + \sigma_c \bar{G}_s) ds \tag{4.7}$$

From above equations, known as Fredholm's integral equation of first kind, σ_c and σ_s can be determined.

Now, the hydrodynamic forces, F , due to oscillation are expressed from Eq. (2.12) as

$$F = -\rho\omega^2 Y \int_c \phi \frac{\partial\phi}{\partial n} ds \tag{4.8}$$

And normalized forces, f , with $\rho\omega^2 Y$ can be divided into two parts, f_c and f_s , finally the added mass and damping can be represented as

$$\text{Added Mass} = \rho f_c, \tag{4.9}$$

$$\text{Damping} = \rho\omega f_s, \tag{4.10}$$

5. Haskind-Newman Relation.

Since, as x tends to positive and negative infinity, the Green function G takes the form of

$$G \sim -i \frac{2\pi}{k_0} \frac{k_0^2 - K^2}{hk_0^2 - hK^2 + K} \cosh h k_0(h-b) \cosh k_0(h-y) e^{ik_0|x-a|} \quad \text{as } |x| \rightarrow \infty, \tag{5.1}$$

$A^\pm(k_0)$ can be represented as

$$A^\pm(k_0) = \frac{2\pi}{k_0} \frac{k_0^2 - K^2}{hk_0^2 - hK^2 + K} \int_c \left(\frac{\partial\phi}{\partial n} - \frac{\partial}{\partial n} \right) \cosh k_0(h-b) e^{\mp ik_0 a} ds \tag{5.2}$$

by comparing Eq. (5.1) with Eq. (2.8).

In the above equation, $A^\pm(k_0)$ is a amplitude function of radiation wave, and is called as Kochin function.

If the arbitrary section is symmetric about y axis, then

$$A^+(k_0) = A^-(k_0). \tag{5.3}$$

The amplitude ratio \bar{A} of the radiation wave at infinity to the motion amplitude is

$$\begin{aligned} \bar{A} &= \frac{\bar{\zeta}}{Y} \\ &= -KA^\pm(k_0) \cosh k_0 h. \end{aligned} \tag{5.4}$$

Damping, N , and the Kochin function have a relation such as

$$\begin{aligned} N &= \rho\omega \frac{k_0}{2} [\sinh k_0 h \cosh k_0 h + k_0 h] \\ |A^\pm(k_0)|^2 & \end{aligned} \tag{5.5}$$

Hence, we can obtain the Haskind-Newman relation from the Eq. (5.4) and Eq. (5.5) in the form of

$$\frac{N}{\rho\omega} = \frac{k_0}{2} [\sinh k_0 h \cosh k_0 h + k_0 h] \left| \frac{\bar{A}}{K \cosh k_0 h} \right|^2 \tag{5.6}$$

6. Numerical Examples

To test the effect of numbers of source distributed on the body surface on the results of calculation of hydrodynamic forces, 11, 21 and 31 singularities are distributed on the surface of a semi-circle in depth-to-draft ratio of 2.0. In this case, the results by 11 points give usable one for the consideration in damping force only, and those by 21 and 31 points are agreeable with those obtained by earlier investigators for both added mass and damping. Considered this property, all results of the present paper have been obtained by distributing 21 point singularities on the immersed body surface.

For the calculation of stream function Ψ and velocity potential Φ ;

$$\begin{aligned} \Phi = & 2\pi \frac{k_o^2 - K^2}{k_o(hk_o^2 - hK^2 + K)} \cosh k_o(h-b) \cosh k_o(h-y) \sin(k_o|x-a| - \omega t) - \sum_{n=1}^{\infty} 2\pi \frac{k_n^2 + K^2}{k_n(hk_n^2 + hK^2 - K)} \cos k_n(h-b) \cos k_n(h-y) e^{-k_n|x-a|} \cos \omega t, \quad (3.6) \\ \Psi = & \text{sgn}(x-a) \left\{ -2\pi \frac{k_o^2 - K^2}{k_o(hk_o^2 - hK^2 + K)} \cosh k_o(h-b) \sinh k_o(h-y) \cos(k_o|x-a| - \omega t) \right. \\ & \left. - \sum_{n=1}^{\infty} 2\pi \frac{k_n^2 + K^2}{k_n(hk_n^2 + hK^2 - K)} \cos k_n(h-b) \sin k_n(h-y) e^{-k_n|x-a|} \cos \omega t, \quad (3.7) \right. \end{aligned}$$

Newton's method was applied to calculate k_o and k_n , and in calculation of infinite series in above equations, truncation of series term was treated by the following condition;

$$\text{EXP}(-k_N|x-a|) < 1.0E-0.6 \quad (6.1)$$

The added mass and damping was nondimensionalized as

$$\bar{\mu}' = \frac{\text{Added mass}}{\rho\pi B^2/8} \quad (6.2)$$

$$\bar{\lambda} = \frac{\text{Damping}}{\rho\omega\pi B^2/8} \quad (6.3)$$

B : Breadth,

and the relation between damping and amplitude ratio can be derived from Eq. (5.6) as

$$\bar{A} = \sqrt{|Kk_o f_s \sinh 2k_o h / (\sinh 2k_o h + 2k_o h)|} \quad (6.4)$$

6.2 Semi-circle

The effect of depth of water on the added mass due to a heaving oscillation was shown in Fig. 3, on damping in Fig. 4. It can be shown that the added mass

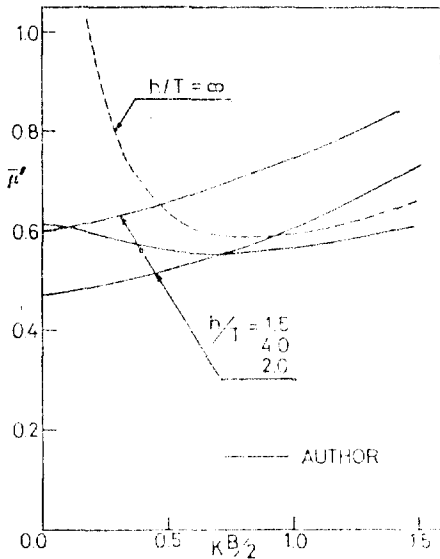


Fig. 3 Added mass for semi-circle in heave

and damping increase as the depth decreases from the above results. And it is noted that the added mass coefficient is becoming larger increasing depth-to-draft ratio in the low wave number region. It is understood from the fact that the added mass coefficient becomes infinity when wave number tends to zero.

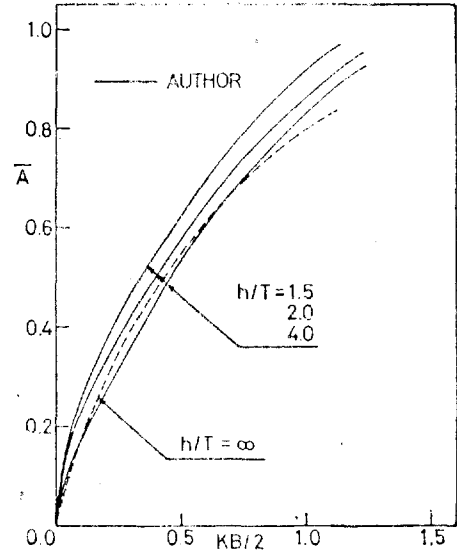


Fig. 4 Amplitude ratio for semi-circle in heave

6.3 Lewis form

From Fig. 5 and 6, it is clear that the behavior of added mass and damping of Lewis form cylinder with a half beam-to-draft ratio, $B/2T$, of 1.0 and a

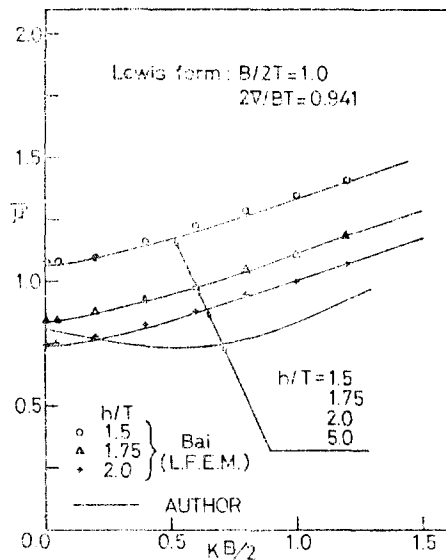


Fig. 5 Added mass for Lewis form in heave

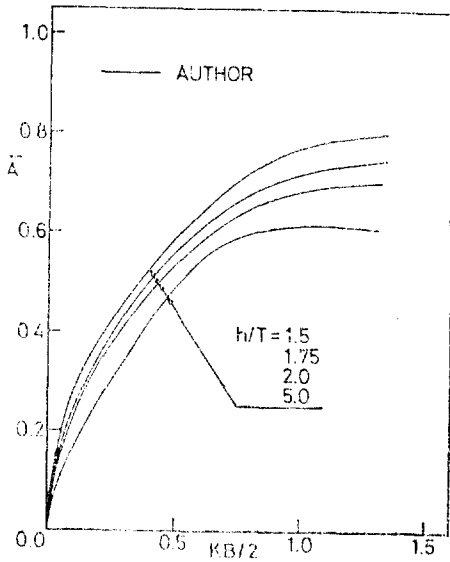


Fig. 6 Amplitude ratio for Lewis form in heave

sectional area coefficient, $2F/BT$, of 0.941 in finite depths is similar to those of a semi-circle. And the shallow water effect on added mass of Lewis form for a heaving oscillation seems to be greater than that of a semi-circle, comparing the Fig. 3 and Fig. 5.

7. Experimental Program

7.1. Model

Principal dimensions of the Lewis cylinder are given in Table 1.

Table 1

Length $L=1.75\text{m}$	Midship area coeff. $\beta=C_m=0.941$
Breadth $B=0.30\text{m}$	Half Beam draft ratio $H=B/2T=1.0$
Depth $D=0.21\text{m}$	Water plane area $A_w=0.525\text{m}^2$
Draft $T=0.15\text{m}$	
Displacement $W=71.1\text{Kg}$	Material Brass

7.2. Experimental Basin

The tests were conducted in the basin of the Institute of Industrial Science, University of Tokyo. The arrangement of the basin is shown in Fig. 8. The dotted line stands for the false bottom for shallow water testing. The carriage on which the forced oscillating apparatus was mounted was located at the midstation of the basin. The radiation waves generated by oscillating model were measured by the resistance

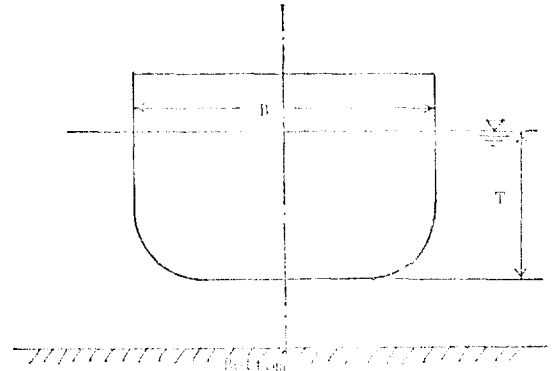


Fig.7 Lewis form model

type wave gauge which was located at 5 meters distance from the model.

7.3. Mode of Oscillation.

The mode of oscillation was heaving only. The amplitude was $\pm 0.01\text{m}$ and the range of frequency between 2.5 Hz and 9 Hz.

7.4. Measurement System

The block diagram of the measurement system is shown in Fig.9. For the measurement of the force, two load cells of tension-compression type were used.

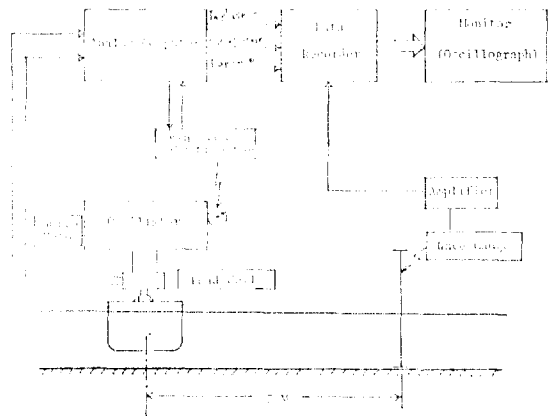


Fig.9 Block diagram of measurement System

7.5. Water of Finite Depth

Three water depths were investigated: $h/T=1.5, 1.75$ and 2.0 , where T is the draft of the model, h water depth.

7.6. Analysis of the Experiment

The equation of heaving motions of the model is written as follows,

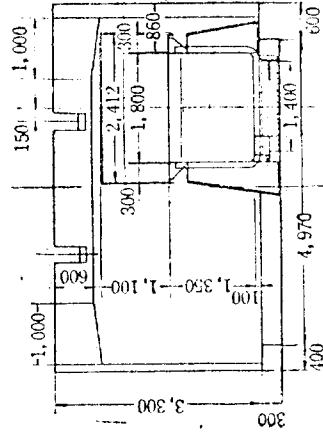
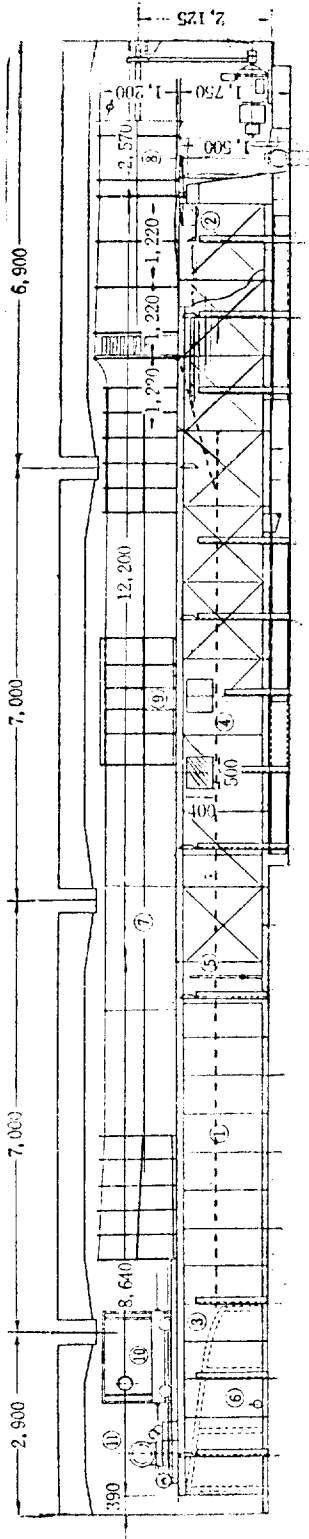


Fig. 8. General arrangement.

- ① Tank
- ② Wave maker
- ③ Wave absorber
- ④ Observation window
- ⑤ Supply pipe
- ⑥ Discharge valve
- ⑦ Wind tunnel
- ⑧ Fan
- ⑨ Transparent panel
- ⑩ Carriage
- ⑪ Driving gear

$$(M+m)\ddot{z} + N\dot{z} + \rho g A_w z = E \tag{7.1}$$

where, $M = \rho V$, $z = z_o \cos \omega t$, $E = E_o \cos(\omega t + \alpha)$

- ρ : density of water
- V : volume
- A_w : water plane area
- g : gravity acceleration
- z_o : amplitude of heaving
- m : added mass
- t : time
- α : phase lag
- E_o : amplitude of exciting force
- N : wave damping coefficient
- ω : angular frequency

Multiply both sides of equation (7.1) by $\cos \omega t$ or $\sin \omega t$ which are the signals through sin-cos potentiometer shown in Fig.9, and integrate it along time t from 0 to n times of period T . Then we get two components of the hydrodynamic forces.

(1) In phase components (phase of acceleration)

$$\int_0^{nT} \{(M+m)\ddot{z} + N\dot{z} + \rho g A_w z\} \cos \omega t dt = \int_0^{nT} E_o \cos(\omega t + \alpha) \cos \omega t dt \rightarrow \{-(M+m)\omega^2 + \rho g A_w\} z_o \frac{nT}{2} = E_o \cos \alpha \frac{nT}{2} \tag{7.2}$$

(2) Out of phase components (phase of velocity)

$$\int_0^{nT} \{(M+m)\ddot{z} + N\dot{z} + \rho g A_w z\} \sin \omega t dt = \int_0^{nT} E_o \cos(\omega t + \alpha) \sin \omega t dt \rightarrow N \omega z_o \frac{nT}{2} = E_o \sin \alpha \frac{nT}{2} \tag{7.3}$$

From equation(7.2) and(7.3), the added mass and wave damping coefficient are obtained as follows,

$$m = \frac{\rho g A_w}{\omega^2} - \frac{E_o \cos \alpha \frac{nT}{2}}{z_o \omega^2 \frac{nT}{2}} - M \tag{7.4}$$

$$N = \frac{E_o \sin \alpha \frac{nT}{2}}{\omega z_o \frac{nT}{2}} \tag{7.5}$$

The relation between wave damping coefficient and wave amplitude ratio is derived from Haskind-Newman's formula;

$$N = \frac{\rho g L \bar{A}^2}{\omega k_o} \left(1 + \frac{2k_o h}{\sinh 2k_o h}\right) \tag{7.6}$$

or

$$\bar{A}^2 = N / \left\{ \frac{\rho g L}{\omega k_o} \left(1 + \frac{2k_o h}{\sinh 2k_o h}\right) \right\} \tag{7.7}$$

where wave amplitude ratio $\bar{A} = \eta / z_o$, η : amplitude of radiation wave and the relation between wave number k_o and angular frequency ω

$$\frac{\omega^2}{g} = k_o \tanh k_o h \tag{7.8}$$

The phase lag α is obtained as follows

$$\tan \alpha = \frac{E_o \sin \alpha \frac{nT}{2}}{E_o \cos \alpha \frac{nT}{2}} = \frac{N \omega}{-(M+m)\omega^2 + \rho g A_w} \tag{7.9}$$

Right hand sides of equation(7.2) and(7.3) can be obtained precisely by making use of a planimeter when experimental data are analysed.

7.7. Experimental Results

Experimental results were represented in dimensionless forms as follows,

$$\text{(added mass)} \quad \bar{\mu}' = m / \rho \frac{\pi}{8} B^2 L$$

$$\text{(wave damping coefficient)} \quad \bar{A}^2 = N \left\{ \frac{\rho g L}{\omega k_o} \left(1 + \frac{2k_o h}{\sinh 2k_o h}\right) \right\}$$

$$\text{(radiation wave amplitude ratio)} \quad \bar{A} = \eta / z_o$$

$$\text{(amplitude of exciting force)} \quad e' = |E| / \rho g z_o B L$$

These results are shown in Fig. 10,11 and 12 respectively. Phase lag is shown in Fig.13. Characteristics of two load cells are little bit different from each other. Only the experiment of water depth $h/T=1.5$ was conducted considering the adjustment of two load cells. The difference between adjustment and non-adjustment of two load cells is shown in Fig'14.

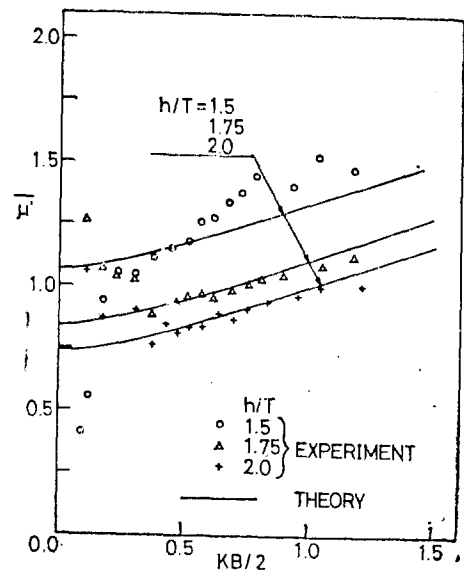


Fig. 10 Added mass for Lewis form

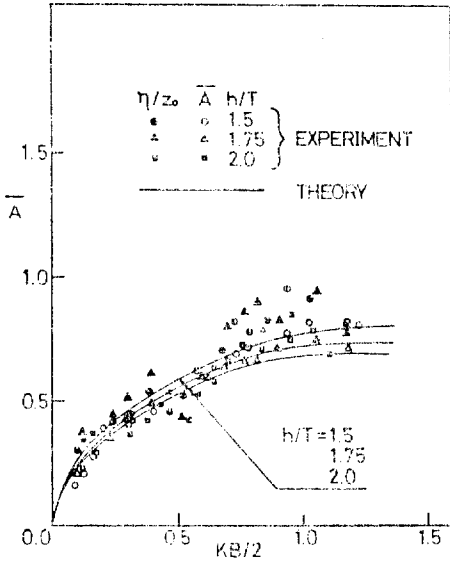


Fig. 11. Amplitude ratio for Lewis form

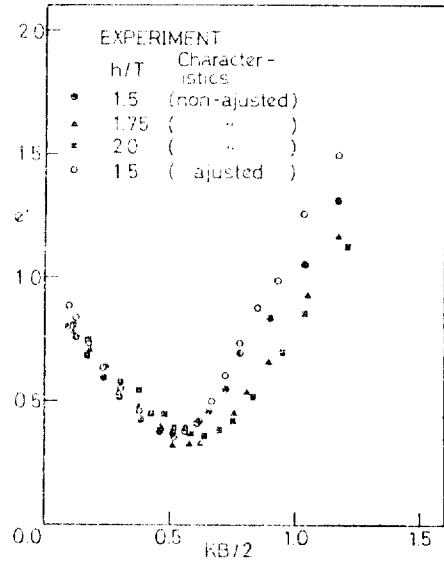


Fig. 12. Amplitude of Hydrodynamic Heaving Force

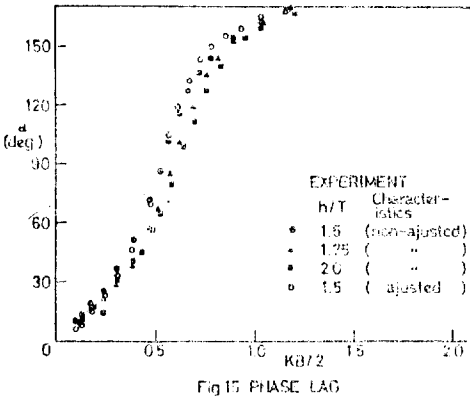


Fig.13. Phase Lag

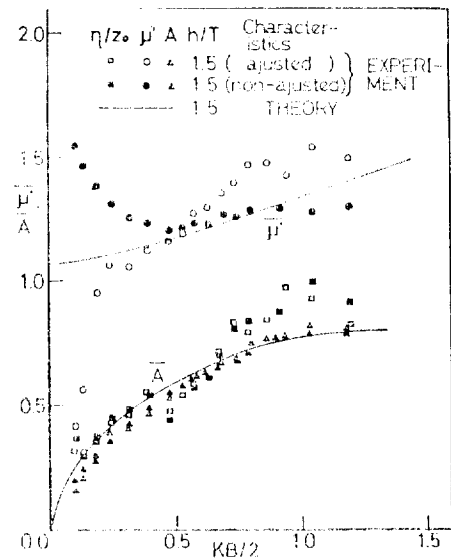


Fig. 14 Difference between adjusted & non-adjusted characteristics of load cells

8. Discussions and results

The results obtained by author's method for a heaving circular cylinder in a depth-to-draft ratio of 2.0 are compared, in Fig. 15 and 16, with those by Bai's Localized Finite Element Method [3], Yeung's Fundamental Singularity Distribution Method [4], Kim's New Multipole Expansion Method, and Yu-Ursell's.

Author's results coincide well with those by Bai and

Yeung, however those by Kim give a small value compared to others in the range of $KB/2 > 1.0$.

In a zero limiting case of a frequency, the added mass by Yu-Ursell's and Kim's increases infinitely, but it is proved by Bai(1976) that the added mass has a finite value as a frequency tends to zero. Keil (1974) and Ursell(1974), also, had obtained the same results by the calculation. In this connection, author's present results are acceptable.

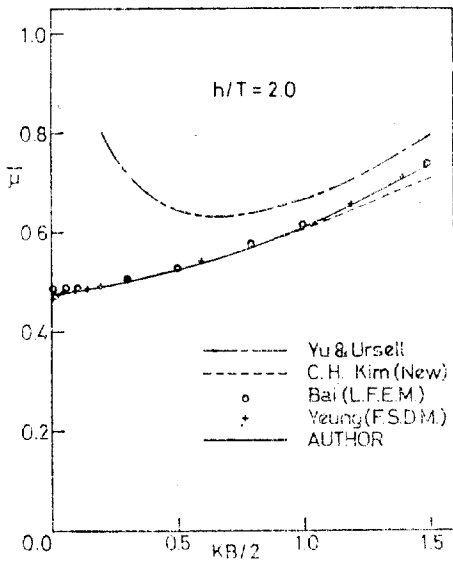


Fig. 15 Added mass for semi-circle in heave

For the Lewis form cylinder with a half beam-to-draft ratio of 1.0 and a sectional area coefficient of 0.941, the experimental results are compared with those by calculation. This reveals that the results by experiment give a little lower value than those by calculation at h/T of 1.75 and 2.0 except low frequency ranges. And it seems that the discrepancy between results by experiment and calculation at the depth of $1.5T$, as shown in Fig. 10 and Fig. 11, is mainly based on difficulties of experiment due to an effect by a disturbance of fluid at shallow water.

Acknowledgement

The authors would like to express their gratitude to Dr. H. Isshiki of the Technical Research Laboratory, Hitachi Shipbuilding and Engineering Co., and Dr. C.M. Lee of the Naval Ship Research and Development Center for their guidance and various discussions during the development of the method.

Thanks are also due to Dr. K.J. Bai of the Naval Ship Research and Development Center for the provi-

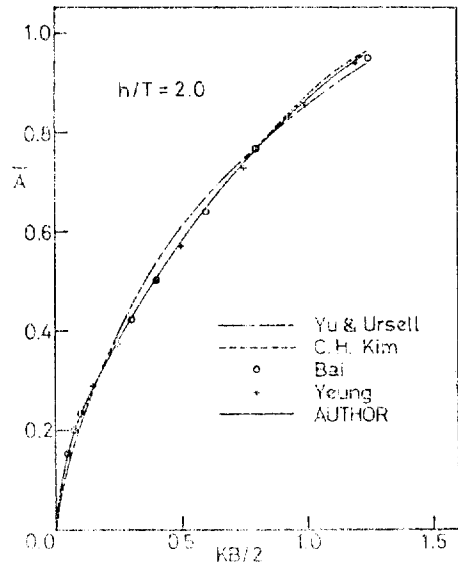


Fig. 16 Amplitude ratio for semi-circle in heave

ding the result of calculation of hydrodynamic forces for Lewis form cylinder by the finite element method for the present paper.

References

- [1] Yu, Y.S. and Ursell, F., "Surface Waves Generated by an Oscillating Circular Cylinder on Water of Finite Depth: theory and experiment", *Journal of Fluid Mech*, Vol. 11, 1961.
- [2] Kim, C.H., "Hydrodynamic Forces and Moments for Heaving, Swaying, and Rolling Cylinders on Water of Finite Depth", *Journal of Ship Research*, Vol. 13, No.2, June 1969.
- [3] Bai, K.J., "A Variational Method in Potential Flows with a Free Surface", *Univ. of Calif. Berkeley, College of Engineering, Rep. NA72-2*, Scpt. 1972.
- [4] Yeung, Ronald W.C., "A Singularity-Distribution Method for Free-Surface Flow Problems with an Oscillating Body", *Ph.D. Dissertation, University of California, Berkeley, California*, Sept. 1973.